

AD-A083 855

NAVAL POSTGRADUATE SCHOOL MONTEREY CA

F/6 8/10

FIRST-GENERATION NUMERICAL OCEAN PREDICTION MODELS -- GOAL FOR --ETC(U)

DEC 79 R L ELSBERRY, R W GARWOOD

NPS-63-79-007

UNCLASSIFIED

NL

1 of 1  
AL 8  
reels



			<div>END DATE FILMED 6-80 DTIC</div>										

✓  
NPS 63-79-007

ADA 083855

**NAVAL POSTGRADUATE SCHOOL**  
**Monterey, California**



DTIC  
ELECTE  
S MAY 6 1980 D  
A

**FIRST-GENERATION NUMERICAL OCEAN  
PREDICTION MODELS -- GOAL FOR THE 1980's**

by

**Russell L. Elsberry**

**Roland W. Garwood, Jr.**

**December 1979**

Approved for public release; distribution unlimited.

Prepared for: **Naval Ocean Research and Development Activity**  
**Office of Naval Research, Ocean Science and Technology**

80 5 6 041

FILE COPY

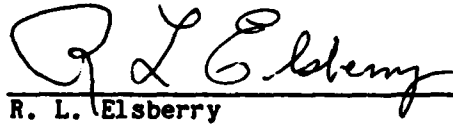
NAVAL POSTGRADUATE SCHOOL  
Monterey, California 93940

Rear Admiral John J. Ekelund  
Superintendent

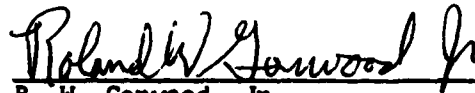
J. R. Borsting  
Provost

The content of this report was developed with the contract support of the Office of Naval Research, Ocean Science and Technology Branch, and of the Naval Ocean Research and Development Activity.

This report was prepared by:

  
R. L. Elsberry

Professor of Meteorology

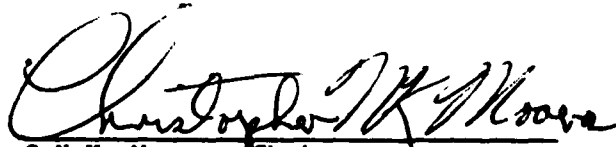
  
R. W. Garwood, Jr.

Assistant Professor of Oceanography

Reviewed by:

  
G. J. Haltiner

Chairman  
Department of Meteorology

  
C.N.K. Mooers

Chairman  
Department of Oceanography

Released by:

  
W. M. Tolles

Dean of Research

Accession For	
NTIS GAAI	<input checked="checked" type="checkbox"/>
DDC TAB	<input type="checkbox"/>
Unannounced	<input type="checkbox"/>
Justification	
By _____	
Distribution/_____	
Availability Codes	
Dist	Availand/or special
A	

Unclassified

SECURITY CLASSIFICATION OF THIS PAGE (When Data Entered)

REPORT DOCUMENTATION PAGE		READ INSTRUCTIONS BEFORE COMPLETING FORM	
1. REPORT NUMBER NPS-63-79-147	2. GOVT ACCESSION NO. AD-A083855	3. RECIPIENT'S CATALOG NUMBER	
4. TITLE (and Subtitle) First-Generation Numerical Ocean Prediction Models -- Goal for the 1980's		5. TYPE OF REPORT & PERIOD COVERED Report for October 1978-December 1979	
7. AUTHOR(s) Russell L. Elsberry and Roland W. Garwood, Jr		8. CONTRACT OR GRANT NUMBER(s)	
9. PERFORMING ORGANIZATION NAME AND ADDRESS Naval Postgraduate School Monterey, California 93940		10. PROGRAM ELEMENT, PROJECT, TASK AREA & WORK UNIT NUMBERS NR083-275-5 N0001479WR90020 NC140 N6846280WR00029	
11. CONTROLLING OFFICE NAME AND ADDRESS Office of Naval Research, Arlington, VA and Naval Ocean Research and Development Agency, NSTL Station, MS 39529		12. REPORT DATE December 1979	
14. MONITORING AGENCY NAME & ADDRESS (if different from Controlling Office)		13. NUMBER OF PAGES 41	
12 43		15. SECURITY CLASS. (of this report) Unclassified	
16. DISTRIBUTION STATEMENT (of this Report) Approved for public release; distribution unlimited.			
17. DISTRIBUTION STATEMENT (of the abstract entered in Block 20, if different from Report)			
18. SUPPLEMENTARY NOTES This report is based on a talk presented at the Geophysical Fluid Dynamics Laboratory, Princeton, NJ during November 1979.			
19. KEY WORDS (Continue on reverse side if necessary and identify by block number) Ocean prediction model Atmospheric forcing of ocean Ocean mixed layer Ocean circulation model			
20. ABSTRACT (Continue on reverse side if necessary and identify by block number) Using the experience of numerical weather prediction during the 1950's and 1960's as a model, a case is presented for development during the 1980's of an ocean prediction capability. Examples selected from recent research at the Naval Postgraduate School are used to illustrate some aspects of the theoretical background, representation of physical processes, observational-support systems and the justification for a first-generation ocean prediction system.			

DD FORM 1 JAN 73 1473

EDITION OF 1 NOV 68 IS OBSOLETE  
S/N 0102-014-6001

Unclassified

3 SECURITY CLASSIFICATION OF THIS PAGE (When Data Entered)

551450

## LIST OF FIGURES

- Figure 1. Ocean temperature distribution predicted using an embedded mixed layer model within an ocean circulation model. Cross-section is aligned along the track of the model storm which was located at 450 km at the initial time and has moved toward the right at  $5 \text{ m s}^{-1}$  and is at 1315 km after 48 h.
- Figure 2. Cumulative percentage of rank-ordered  $3 \text{ h } u_*$ ,  $u_*^3$  and  $Q_a$  values versus cumulative percentage of observations based on 24-, 15- and 23-year samples (September to December) at OWS P, V and N, respectively.
- Figure 3. Daily-averaged values of (A) sea-surface temperature, (B) mixed layer depth, (C) insolation ( $Q_s$ ) and surface heat flux plus back radiation ( $Q_a$ ), and (D)  $u_*^3$  at OWS P during 1963. Dashed lines represent the long-term mean (24 year) values.
- Figure 4. Similar to Fig. 3 except at OWS V during 1959.
- Figure 5. Model-predicted maximum daily depths of the well-mixed layer (solid), surface temperature minus  $0.2^\circ\text{C}$  (top of shaded), surface temperature minus  $1.0^\circ\text{C}$  (top of cross-hatching) and surface temperature minus  $2.5^\circ\text{C}$  (bottom of cross-hatching) during 1959 at OWS P.
- Figure 6. Wind speed, total heat flux and solar heat flux at  $32\text{N}$ ,  $175\text{W}$  during 1977 extracted from FNOC atmospheric model analyses and 12 h predictions.

- Figure 7. Location of TRANSPAC ship-of-opportunity bathythermograph observations during March and April 1977 (provided by W. White and R. Bernstein).
- Figure 8. Heat content ( $10^4$  cal  $\text{cm}^{-2}$ ) relative to the 200 m temperature calculated along  $175^\circ\text{W}$  from TRANSPAC analyses in September (solid) and November (dashed) 1976. Vertical bars indicate the cumulative surface heat flux between 15 September and 15 November 1976.
- Figure 9. Initial (circles) temperature profiles at (a)  $38^\circ\text{N}$ ,  $165^\circ\text{W}$  and (b)  $32^\circ\text{N}$ ,  $175^\circ\text{W}$  from September 1976 TRANSPAC analysis and mean predicted values at 10 m intervals for months of October (triangle), November (horizontal dash) and December 1976 (cross). Verification data from December 1976 TRANSPAC analysis are given at 0, 30, 60, 90, 120, 150 and 200 m (diamond).
- Figure 10. Model-predicted layer (a) depth and (b) temperature during 1976 along  $38^\circ\text{N}$ . Initial spacing between the traces at each longitude are 100 m and  $2^\circ$ , respectively.
- Figure 11. Composite of model-predicted mixed layer temperature (upper) and depth (lower) for 6 longitudes as in Fig. 10, relative to spring transition date (zero day).
- Figure 12. Composite of atmospheric forcing parameters relative to spring transition date as in Fig. 11. Wind speed, total heat flux and solar heat flux are extracted from FNOC atmospheric model analyses and 12-h predictions.

Figure 13. Model-predicted mixed layer depth and temperature as in Fig. 10 except along 155W during 1976.

Figure 14. Model predictions as in Fig. 9 except at 30N, 175W and for March (circle), April (triangle), May (horizontal dash) and June (cross) 1977. Verification data are from June 1977 TRANSPAC analysis. (a) Unmodified surface heat flux and (b) reduction of upward heat flux by  $10 \text{ cal cm}^{-2} \text{ h}^{-1}$ .

## 1. Introduction

One often hears that oceanography is several years behind meteorology. Many developments in physical oceanography parallel or build upon the earlier work in meteorology because of the similarity in the dynamics. It is useful to assess the stage of development of the oceanographic endeavor by comparison with the progress in meteorology. The example to be illustrated in this talk<sup>1</sup> is the development of a capability for ocean prediction using numerical methods.

The theme of this talk is that the next decade will see the development of a dynamic ocean prediction system comparable to that of the numerical weather prediction system developed during the 1960s. Development of an oceanic prediction system is a multi-faceted problem. Here, we pursue some aspects of the necessary theoretical background, representation of physical processes, observational-support systems and justification for an ocean prediction system. We limit our discussion to open-ocean regimes and thus avoid the especially complex circulations in coastal regions. In addition, we limit our choice of examples of research-in-progress to our group at the Naval Postgraduate School. Our intention is to use these examples (those of other groups could also be used) as illustrations of the progress toward an operational ocean prediction system. By analogy with the evolution of numerical weather prediction, it seems evident that the building blocks have been laid for development of a comparable ocean system. Justification for the system lies in the deployment of

---

<sup>1</sup>This paper is based on a seminar presented at the Geophysical Fluid Dynamics Laboratory, Princeton, New Jersey, on 3 November 1979.



antisubmarine systems the U. S. Navy, conduct of fisheries management as guided by the Department of Commerce and perhaps also in climate research.

It is not our purpose here to discuss the gaps in our knowledge that must be filled if an operational model is to be produced. Much research and development, many talented workers and considerable computer resources will be required to accomplish the task. As during the development of numerical weather prediction, there will be exciting and rewarding research opportunities as observationalists and modelers work toward a common goal.

## 2. Theoretical background

The basis for numerical weather prediction (NWP) was established in Princeton, NJ, at the Institute for Advanced Studies (e.g. Platzman, 1979), but the development of operational numerical weather prediction models required years of additional research. Certainly the success of atmospheric general circulation models (GCM) at the Geophysical Fluid Dynamics Laboratory and other places was an important step in demonstrating the feasibility of NWP models. Such factors as numerical stability over long integration periods and the representation of physical processes in the GCM were necessary building blocks.

Continuing this analogy with atmospheric models, the numerical simulations of the global ocean (see review by Haney, 1979), as well as the eddy scales, would seem to provide a similar demonstration of feasibility for ocean prediction. However, nearly all of these models have been driven with constant or slowly-varying forcing. The ocean mixed layer serves as a buffer zone between the atmospheric forcing and deep circulation. To resolve properly the range of time scales induced by realistic atmospheric forcing, we will require an ocean model that

includes both mixing and advective processes. One-dimensional mixing models simulate a major fraction of the upper ocean response to atmospheric storms (cf. Camp and Elsberry, 1978). Consequently, the recent advances in mixed layer theory (see review by Garwood, 1979) are an essential component. However, there are other examples in which advective effects can not be neglected.

One of the chief problems in coupling the mixed-layer models and the ocean circulation models is the difference in time and space scales. Whereas mixed layer models typically use time steps of 1 h and vertical increments of 1 to 3 m, the oceanic GCM may use time steps of many hours and may have layers 10 to 100 m thick. The approach at the Naval Postgraduate School has been to embed the bulk, turbulent closure model of Garwood (1977) within the vertical structure of the oceanic GCM of Haney (1980). An example (see Adamec, et al 1978, 1979) of the simulations which may be achieved with such a coupled model is shown in Fig. 1. Only the upper 600 m of the solution is displayed. A total of 25 layers ranging in thickness between 6 m near the surface and 100 m has been used over the 1000 m depth. A case of hurricane-ocean interaction is chosen because of the strong advective and mixing effects to be expected. A stress pattern typical of a hurricane has been moved from an initial point at 450 km to 1315 km after 48 h. As expected for a hurricane moving at  $5 \text{ m s}^{-1}$ , a large amplitude oscillation is set up on the thermocline. Isotherms within the thermocline are first displaced downward as the storm center approaches. Following the storm passage, there is a rapid upwelling, with the  $17.2^{\circ}\text{C}$  isotherm being raised from around 200 m to about 105 m. Regions of large horizontal temperature gradients are produced in advance and behind the cold upwelled water. These thermocline oscillations would

continue for several inertial periods before being damped. There is a net temperature decrease near the surface due to the upward heat flux to the storm and the mechanical mixing induced by the strong winds. Even though the wind speed is decreasing after the storm center passes, cooling continues as the upwelling brings cold water nearer the surface where mixing is effective.

The purpose of showing such an extreme example as hurricane-ocean interaction is to demonstrate that realistic advective and mixing effects can presently be simulated in a coupled ocean model. A relatively fine grid and detailed atmospheric forcing would be required to attempt a prediction with real data. Before developing such a complex model, it will be necessary to begin with simpler models. The "first-generation" model will probably be a mixed layer model only. The purpose of these models will be to predict ocean thermal structure changes in response to atmospheric forcing on time scales of days to weeks. In the following sections, we will describe the physical processes, the atmospheric forcing and the ocean observations necessary to run these first-generation models.

### 3. Representation of physical processes

One of the first prerequisites for atmospheric prediction was the proper representation of the processes involved in extratropical cyclogenesis. By the 1960's, there was ample theoretical background for demonstrating the length and time scales required for prediction of this phenomenon. It was also important to develop a representation of the internal energy redistribution and frictional effects acting on these time scales. We still have much to learn about the release of latent heat in clouds of different scales and the interaction with the atmosphere boundary layer, especially in the tropics. There is little doubt that

attempting to develop an ocean prediction model will also uncover some physical processes which will likely require additional years of research to model properly.

The first-generation ocean mixed-layer models will take advantage of a separation of time scales. That is, the vertical mixing processes on time scales of a few days dominate the advective effects over much of the ocean. Thus the principal physical process to be represented is the redistribution of the density structure induced by vertical mixing processes. If the upper ocean is well mixed to a depth  $Z = -h$ , the vertical temperature flux within the layer will be a linear function of depth. Given the surface heat flux, the problem is to determine the vertical temperature flux at the base of the mixed layer. As shown by Niiler and Kraus (1977), this vertical temperature flux can be written in terms of an entrainment velocity  $w_e$  at the mixed layer base.

One of the important factors influencing  $w_e$  is proportional to the third power of the atmospheric friction velocity ( $u_*^2 = \tau \rho^{-1}$ ). The distribution of  $u_*^3$  values is very skewed, as shown in Fig. 2. In this diagram, the three-hourly observations at ocean weather ships have been rank-ordered and accumulated (see details in Elsberry and Camp, 1978; Elsberry and Raney, 1978). For example, 50 percent of the smallest values of  $u_*^3$  throughout the entire record contribute only 15 percent of the total accumulated value. The remaining 50 percent of the total rate of working on the upper ocean by the wind occurs during a few large wind speed events, lasting less than 15 percent of the time. These are associated with the passage of extratropical cyclones. This type of distribution occurs during both winter and summer seasons. It is remarkable that the same curve fits the  $u_*^3$  distribution for the three

ocean weather ship locations (P: 50°N, 145°W; N: 30°N, 140°W; V: 34°N, 164°E) shown, especially considering the large differences in the total  $u_*^3$ . The distribution of the upward heat flux at the ocean surface ( $Q_a$ ) is not as skewed, as it follows the  $u_*$  (or wind speed) distribution. The  $Q_a$  is a part of the buoyancy flux that also contributes to the entrainment velocity at the base of the layer, if the heat flux is upward. The convective overturning of parcels contributes to the turbulent energy available for mixing at the base of the layer.

Daily values of  $u_*^3$ , solar flux ( $Q_s$ ) and  $Q_a$  at OWS P are shown in Fig. 3. As indicated above, the  $u_*^3$  trace is characterized by a background of small values with much larger values of brief duration at 3-4 day intervals. There is also a synoptic period variability in  $Q_s$  and  $Q_a$ . The oceanic response to this atmospheric forcing is shown in terms of the sea-surface temperature and mixed-layer depth. From the beginning of September until about 10 October 1963, the temperatures were higher than the long-term mean. A major fraction of the seasonal decrease in sea-surface temperature then occurs over the next 10 to 15 days, and the temperatures remain below normal for the remainder of the year. The daily-averaged, mixed-layer depth trace is about 10 m shallower than the long-term mean prior to 10 October 1963. The layer deepens rapidly during the period of large  $u_*^3$  values, and remains deeper than normal throughout November 1963.

We also consider the periods of light winds to be important in determining the oceanic thermal response to atmospheric forcing. An example of the distributions of  $u_*^3$ ,  $Q_s$  and  $Q_a$  at OWS V during January to August is shown in Fig. 4. The large variability in  $u_*^3$  relative to the long-term mean is again shown. Note that there is a period from around 15

March to 15 April during which the mean  $u_*^3$  decreases significantly. The summer-time values are considerably smaller, although there continues to be synoptic-period variability. During the same period that the wind speeds are decreasing, the solar flux is increasing. A net downward heat flux tends to oppose deepening of the layer. If there is insufficient wind mixing to maintain the depth against the stabilizing influence of the surface heating, the layer will become shallower. This tends to occur throughout the year during the low wind speed periods between the passage of storms, as shown in both Figs. 3B and 4B. Likewise, the period of maximum daytime heating will lead to a similar shallowing of the layer if the wind speed is not large enough to maintain layer depth. A very rapid transition in mixed-layer depth occurs around 1 April 1959. Prior to this time, the depth was around 130m. During a single diurnal period, the layer depth decreased to 40 m. Although the passage of subsequent storms temporarily increased the layer depth, the values did not approach the winter-time values. The effect on the sea-surface temperature is to trap the heat flux in a shallower layer, and thus increase the temperature. If the layer is very shallow, the rate of temperature increase can be quite large. Elsberry and Garwood (1978) have shown that warm and cold anomalies in the upper ocean throughout the summer can result from early and late transition dates, respectively.

The important feature of these data sets is that the oceanic mixed layer depth and temperature do not smoothly change in time. Rather the evolution tends to respond directly to the frequency and intensity of storm events. Rapid cooling and deepening occur during high wind speed periods associated with storms, especially if there is upward heat flux.

Warming and shallowing tend to occur during light wind speed periods with downward heat flux.

It is important to determine whether an oceanic mixed-layer model can predict these changes in the ocean thermal structure given the atmospheric forcing. An example (Garwood and Adamec, 1980) of a long-term simulation with the 3 h forcing at OWS P is shown in Fig. 5. The Garwood (1977) model was started from the observed temperature on January 1. This is the only ocean thermal structure observation used, although the observed sea-surface temperature has been used to calculate the surface heat fluxes. The simulated isothermal depths during winter indicates considerable variability as in Fig. 3. A rapid transition to a shallow depth is predicted about day 100, after which the layer remains above 65 m. Formation of the seasonal thermocline and its associated stability (temperature intervals relative to the surface temperature) are shown in Fig. 5. The autumn storms then gradually erode the layer. Mixed-layer depth observations (not shown) exhibit the large-scale trends and much of the short-term variability shown in the simulation.

#### 4. Specification of atmospheric forcing

The ocean mixed-layer model requires hourly estimates of wind speed, solar flux and total surface heat flux (if the salinity effects were included in the model, the precipitation rate would also be required). In the above examples, the atmospheric forcing was provided from 3 h observations at the ocean weather ships. It is thus an important question whether or not the atmospheric forcing can be provided at the required frequency over the ocean away from the weather ships (only a few of which remain in existence). A key premise in our research at the Naval Postgraduate School is that this atmospheric forcing can be derived from the Fleet

Numerical Oceanography Center (FNOC) atmospheric analysis/prediction models. Synoptic-scale wind fields are analyzed each 6 h and the atmospheric prediction models include hourly calculations of the surface heat budget over the ocean. Are these atmospheric model-derived fields adequate for ocean prediction?

The present FNOC analyses of wind over the ocean make use of ship reports and satellite-derived cloud motion vectors. In many areas, there is adequate coverage to define the synoptic-scale variability. In other areas, the data coverage is poor, and there is reasonable doubt as to the validity of the analyses. A number of possibilities are being explored to enhance the observations of wind over the ocean. These include satellite-based instruments (such as on SEASAT) and over-the-horizon radar. If these instruments are to be useful for ocean prediction, they must be able to identify the oceanic regions of both high and low wind speeds. Given an accurate analysis of the wind field, the atmospheric model must provide the correct prediction of the winds with time.

The components of the surface heat budget include the latent and sensible heat fluxes and the incoming and outgoing radiative fluxes. There are inadequate ship observations over the oceans to calculate these variables on the required (hourly) time scales. There are again a number of existing and proposed satellite instruments which may increase our capability to specify the heat flux components. One of the most difficult of the variables to observe remotely will be the latent heat flux, which depends on the near-surface specific humidity. For the present, we use the FNOC atmospheric model-derived heat fluxes (U.S. Naval Weather Service, 1975). The sensible and latent heat fluxes are calculated from bulk aerodynamic equations given the sea-surface temperature distribution.



Friehe and Pazan (1978) found good agreement between the FNOC winds and heat fluxes using independent observations over a two-week period. One of the more questionable aspects of the model heating package is the estimate of the cloud amount which is used in the radiation calculations. In the present formulation, cloud cover is simply related to the relative humidity in the column.

An example of the time series of atmospheric forcing derived from the FNOC fields is shown in Fig. 6. The wind speeds are derived from the 6 h analyses using a cubic spline interpolation. Although the heat flux values are presently being archived at 6 h intervals, during the period shown the values were only available at 12 h intervals (details of the extraction and interpolation routines can be found in Gallacher, 1979). The wind and heat flux values derived from the FNOC fields appear to contain the synoptic-scale variability shown above to be important for ocean prediction. They do not contain the mesoscale variability that would be expected from point measurements. One measure of the suitability of these fields is the performance of the ocean model.

#### 5. Ocean thermal structure observations/predictions

One of the primary reasons why ocean prediction has lagged behind atmospheric prediction has been the paucity of ocean observations. The global rawinsonde network with 12 h releases has been adequate, especially over land areas, to resolve the primary synoptic-scale atmospheric features. The time scales of the oceanic flow are considerably longer than in the atmosphere. However, the comparable space scales for baroclinic motion in the ocean are several orders of magnitude smaller than in the atmosphere. This requirement for observations on very small space scales will remain the greatest obstacle to ocean circulation

prediction. However, there are larger scale anomalous thermal structure features with space scales comparable to atmospheric cyclones. These ocean features are the object of research of the North Pacific Experiment (NORPAX). White and Bernstein (1979) have designed a ship-of-opportunity expendable bathythermograph (XBT) program called TRANSPAC for observing ocean thermal structure on space scales of a thousand or more kilometers. An example of the TRANSPAC data coverage for a month is given in Fig. 7. Although there are considerable gaps near the coasts, there are enough data in the central Pacific to define the thermal structure over a 15-20° latitude band. Haney (1980) has used the TRANSPAC data in simulation experiments with an ocean circulation model that are designed to test anomaly generation hypotheses. Because all TRANSPAC observations within a particular month are used in the analysis, this defines the time scale for the initialization and verification of the ocean model.

A one-dimensional, mixed-layer model considers only the vertical fluxes of heat. Consequently a necessary condition for accurate model predictions is that the change in heat content from the ocean analyses must be nearly equal to the surface heat flux. A check (Elsberry, Gallacher and Garwood, 1979) of this condition using the TRANSPAC ocean temperature analyses and the FNOC surface heat fluxes is shown in Fig. 8. The heat content in the upper 200 m along 175°W has been calculated relative to the 200 m temperature, which tends to remove the effect of vertically coherent fluctuations that may be related to non-mixing processes. Over most of the latitudinal band, there is a large decrease in heat content from September to November 1976. The vertical lines indicate the integrated total heat flux between 15 September and 15 November 1976 calculated from the FNOC fields. North of 36°N there is

very good consistency between the two calculations. There is clearly disagreement between the surface fluxes and heat content changes south of  $36^{\circ}\text{N}$ , but one can not determine which calculation is in error from these data alone.

Simulations with the Garwood (1977) model in the two regions noted above are shown in Fig. 9. The initial (September) temperature profile at  $38^{\circ}\text{N}$ ,  $175^{\circ}\text{W}$  is rather unusual in that it has a mixed layer depth that is less than 10 m. The predicted October profile illustrates the large temperature decreases near the surface and temperature increases at the base of the layer expected with strong vertical mixing. Further cooling and deepening of the mixed layer is predicted from October to November and into December. The model prediction is in close agreement with the December TRANSPAC analysis. Agreement between surface fluxes and heat content change, plus the correct vertical temperature distribution, indicates that the parameterization of surface mixing processes is capable of accounting for the thermal structure. A similar prediction at  $32^{\circ}\text{N}$ ,  $175^{\circ}\text{W}$  does not verify well. Although the largest discrepancy is found in the upper 100 m, the TRANSPAC values are consistently warmer than the model prediction throughout the upper 200 m. As discussed above in relation to Fig. 8, it is not clear whether the TRANSPAC analyses or the surface fluxes derived from the FNOG fields are in error in this region. There are two other possible explanations. The mixed-layer model may need to be adjusted for different conditions, or the one-dimensional models may not contain the necessary physics. In particular, a horizontal or vertical advective process that is not included in the model could possibly explain the deviations.

During the spring, the important feature to be predicted is the formation of the seasonal thermocline (see Figs. 4 and 5). The monthly TRANSPAC analyses have inadequate time resolution to verify the rapid transition predicted by the mixed-layer model. Examples of the mixed layer depth and temperatures at various longitudes along  $38^{\circ}\text{N}$  are shown in Fig. 10. These simulations with the Garwood model are driven by the time series of atmospheric forcing derived from the FNOC fields and are started from the March TRANSPAC analysis. The predicted mixed layer depth traces show considerable time and space variability. The transition to a shallow layer characteristic of summer conditions occurs before day 105 at longitude 215 ( $135^{\circ}\text{W}$ ). Apparent transitions occur at the other longitudes within a few days of this date - with some appearance of a lag in time as one proceeds eastward. Over the next 10 days, the mixed-layer temperature begins to increase. However, increased mixing occurs subsequently that is sufficient to eliminate the warm, shallow layer between  $175^{\circ}\text{E}$  and  $165^{\circ}\text{W}$  (longitudes 175 and 195 in the figure, respectively). The accumulated heat is then spread over greater than 100 m and the surface temperature decreases. Around day 130, the mixed layer again shallows in the westernmost traces and then remains above 60 m for the remainder of the period. The associated mixed-layer temperature traces increase rapidly following the transition to shallow mixed-layer depths (see Fig. 10b), much as in Fig. 4b. One can see from the space between adjacent temperature traces that the time of transition as well as response to the later forcing events causes horizontal variability along the latitudinal section. Similar variability is predicted along other latitudinal and longitudinal sections (not shown).

It is of interest to explore what features of the atmospheric forcing are most relevant to these predictions of spring transition. Because the transition date varies at each position, the atmospheric forcing was composited for 10 days prior and 20 days following the transition date. The resulting composites of mixed-layer temperature depth for the six longitude traces in Fig. 10 are found in Fig. 11. The day-to-day variability in mixed-layer depth prior to transition contrasts markedly with the smaller mean value and variability following the transition. One can also note a distinct change in the rate of mixed-layer temperature increase with time across the transition date. The composites of the forcing variables are shown in Fig. 12. It is clear that the mean wind speed on the day of transition is much lower than during the 10 days prior to this date. Although the mean wind speed increases slightly during the next few days, the average wind speed over the 20 days following the transition remains smaller than before transition. Such an extended period with less wind mixing (recall this term is proportional to the cube of the wind speed) is required for the warm stable layer to become well established near the surface. The variations in solar radiation derived from the FNOC fields do not seem to be very well correlated with the transition date. The overall trend is toward increasing values. However, the maximum values appear to be modulated by a synoptic-period variability which is larger than the difference in peak values from before to after the transition date. Similar comments apply for the total heat flux trace, except that the nighttime upward heat fluxes are smaller after transition. This is consistent with the smaller wind speeds found during this period. One then finds a trend toward larger net downward heat flux across the transition date, which contributes to the increased warmer temperature. However, it appears from

these composites that the major factor in the transition is the distinct decrease in wind speed for an extended period of time.

It should be emphasized that the net downward flux of heat is a necessary requirement for the occurrence of a transition, and the establishment of a seasonal thermocline. A cross-section of mixed-layer depths and temperatures along  $175^{\circ}\text{W}$  during the spring as predicted by the Garwood model is shown in Fig. 13. There is again a pronounced reduction in variability in mixed-layer depth between the early and later periods for all latitudes north of  $36^{\circ}\text{N}$ . At these latitudes, the mixed-layer temperatures increase rapidly following the transition dates as was the case in Fig. 10b. However, the mixed-layer temperature does not increase at latitudes south of  $36^{\circ}\text{N}$ . In fact, the temperature at  $30^{\circ}\text{N}$  continues to decrease slowly throughout the period. The evolution of the temperature profile at  $30\text{N}$ ,  $175\text{W}$  is given in Fig. 14a. The initial profile is taken from the March 1976 TRANSPAC analysis. It is clear that the model did not predict the formation of a seasonal thermocline as indicated in the verifying data from the June 1976 TRANSPAC analysis. As noted above, the prediction was for continued cooling of the upper layer. One explanation for this trend was the absence of a net downward flux in the derived atmospheric forcing (recall that an excessive upward heat flux in these latitudes was also found during the fall period in Fig. 8). An experiment was run in which the upward heat flux was reduced by  $10 \text{ cal/cm}^2$  during each hourly time step. The model then predicted the development of a seasonal thermocline which is quite reasonable in terms of the verifying data (see Fig. 14b). It thus appears that relatively small bias in the total heat flux can have an important impact on the correct prediction of the magnitude of the seasonal thermocline. If it is indeed a bias in the FNOG heat flux, which is the problem

in these latitudes, it may not have serious consequences for the atmospheric predictions since the atmospheric model is not run for extended periods without new data for correcting the temperature and moisture profiles.

The capability of an ocean model to provide time series of realistic thermal structure profiles given the correct boundary conditions is very important. An example is the long-term integration of the Garwood model with the ocean weather ship data shown in Fig. 5. In many regions of the ocean, there will be long periods without new observations. Without a prediction model, the only option is to revert toward a climatological profile. If one had confidence in the calculations of the local heat budget and the wind forcing, it would be possible to use the mixed layer model to update continually the ocean thermal structure until new observations obtained. It appears that an analysis-prediction-analysis cycle, as used for the atmosphere, would be a useful alternative to a system that simply reverts to climatology in the absence of new observations. This approach would only apply in oceanic regions where vertical mixing processes are dominant. In other regions, the prediction model would have to include advective effects.

#### 6. Justification for ocean prediction models

Given that one has the potential to predict some phenomena, it is still necessary to justify economically the costs of developing and running the model. In the case of weather prediction, there are tremendous economic benefits because of the direct effects on the lives of people everywhere. The justification may be less dramatic in the ocean case, but a few possibilities should be mentioned. (1) Knowledge of the heat storage and distribution in the upper ocean may help us understand

our climate on time scales beyond a few weeks. Whereas we have only considered here the response in the upper ocean to atmospheric forcing, understanding our climate may involve feedback between the ocean and atmosphere, requiring coupled atmospheric-ocean models. Demonstrating that the ocean prediction model can correctly predict the ocean response to given atmospheric forcing, however, seems to be a necessary first step to interactive models. (ii) The National Marine Fisheries Service could use knowledge of the ocean thermal structure to improve fisheries management. (iii) The U.S. Navy is a primary customer for an ocean prediction model because the detection of enemy submarines by acoustical methods requires knowledge of the ocean thermal structure. The Navy has recently organized the Naval Oceanographic Research and Development Activity (NORDA) to provide the link between ocean research and the application in the fleet. The Numerical Modeling Group at NORDA has been tasked to test and develop an ocean analysis and prediction model. With the establishment of this group, and the anticipated computer upgrade at FNOC, which will be required to run such a model, it appears that the Navy has the organization structure and resources to bring an operational ocean prediction model into reality.

## 7. Summary

We have used the experience in numerical weather prediction as a framework for discussing the potential development of a limited ocean prediction capability during the 1980's. We have used some recent research results at the Naval Postgraduate School to illustrate some of the aspects that must be treated if an ocean model is to be integrated with real data and forcing.



(i) An ocean model that is to be driven with real atmospheric forcing must respond on a wide range of time scales. Ocean circulation models with embedded mixed layers are being developed by several groups for this purpose. The ability to treat both advective and mixing processes will be a prerequisite for predicting phenomena such as ocean fronts.

(ii) A knowledge of the wind forcing during storms as well as during extended periods of low wind speeds is necessary to predict properly significant changes in ocean thermal structure. We presently have analyses of the synoptic-scale variability in the wind forcing over the shipping lanes. Further information from the data-sparse regions may be derived by remote sensing systems. In the predictive mode, the ocean model will be limited to the length of time that accurate wind fields can be predicted.

(iii) Over large regions of the oceans there is an approximately local heat balance. This will permit "first-generation" models that are one-dimensional. Various ocean mixed-layer models have the capability of predicting the first-order changes in the ocean thermal structure given the correct forcing. These models need to be compared over a range of time scales and ocean conditions to select a candidate for the first-generation model.

(iv) The mixed-layer models require a specification of the solar radiative as well as the total heat flux during the prediction period. It is proposed that the heating package of the atmospheric prediction model be used as an indirect representation of the thermal forcing. Further comparisons, such as in Friehe and Pazan (1978), of the model-derived heat flux components with point observations should be made.

(v) One benefit of an ocean prediction system lies in providing a better representation of the existing ocean thermal structure in data-sparse regions. An analysis-prediction-analysis cycle will carry forward information from limited observations. If the ocean model includes advective processes, the information from data-rich areas will be propagated into adjacent regions.

It is anticipated that the development of an ocean prediction model will reveal many shortcomings in our knowledge of ocean processes. This will provide a stimulating environment for research and development efforts in all areas related to an ocean analysis and prediction model. Likewise, we will learn more about the data requirements necessary for accurate predictions and thus be able to deploy our limited resources more efficiently. If the experiences of numerical weather prediction are indicative, the decade of the 1980's should be an exciting period as ocean prediction models are developed.

#### Acknowledgements

The authors would like to acknowledge the contribution of their associates especially R. L. Haney, D. Adamec and P. C. Gallacher. Prof. C. Mooers provided helpful comments on the manuscript, which was typed by Ms. M. Marks. The research described here was sponsored by the Office of Naval Research, Ocean Science Branch under contract number NR083-275, N00014-79-WR-90020 and by the Naval Oceanographic Research and Development Activity (Code 320) under contract number N68462-79-WR-90029.

## REFERENCES

- Adamec, D., R. L. Elsberry, R. W. Garwood, and R. L. Haney, 1978: Developmental experiments to include vertical mixing processes in numerical model simulations of ocean anomalies. Presented at Annual Fall Meeting, AGU, San Francisco. Trans. Am. Geophys. Union, 59, 1115.
- Adamec, D., R. L. Elsberry, R. W. Garwood, and R. L. Haney, 1979: Thermal and dynamic response of a model ocean with a mixed layer to hurricane forcing. Presented at Twelfth Technical Conference on Hurricanes and Tropical Meteorology, New Orleans. Bull. Am. Meteor. Soc., 59, 1546.
- Camp, N. T., and R. L. Elsberry, 1978: Oceanic thermal response to strong atmospheric forcing. II. Simulations with mixed layer models. J. Phys. Oceanogr., 8, 215-224.
- Elsberry, R. L., and N. T. Camp, 1978: Oceanic thermal response to strong atmospheric forcing. I. Characteristics of forcing events. J. Phys. Oceanogr., 8, 206-214.
- Elsberry, R. L., P. C. Gallacher, R. W. Garwood, Jr., 1979: One-dimensional model predictions of ocean temperature anomalies during Fall 1976. Naval Postgraduate School Technical Report NPS 63-79-003, 30 pp.
- Elsberry, R. L., and R. W. Garwood, 1978: Sea-surface temperature anomaly generation in relation to atmospheric storms. Bull. Am. Meteor. Soc., 59, 786-789.
- Elsberry, R. L., and S. D. Raney, 1978: Sea-surface temperature response to variations in atmospheric wind forcing. J. Phys. Oceanogr., 8, 881-887.

- Gallacher, P. C., 1979: Preparation of ocean modeling parameters from FNWC atmospheric analyses and model predictions. Report NPS 63-79-005, Naval Postgraduate School, Monterey, CA, 24 pp.
- Garwood, R. W., Jr., 1977: An oceanic mixed layer model capable of simulating cyclic states. J. Phys. Oceanogr., 7, 455-468.
- Garwood, R. W., 1979: Air-sea interaction and dynamics of the surface mixed layer. Rev. Geophys. Space Physics, 17, 1507-1524.
- Haney, R. L., 1979: Numerical models of ocean circulation and climate interaction. Rev. Geophys. Space Physics, 17, 1494-1507.
- Haney, R. L., 1980: A numerical study of the formation of upper ocean thermal anomalies during fall and winter of 1976-77. J. Phys. Oceanogr., 10.
- Niiler, P. P., and E. B. Kraus, 1977: One-dimensional models of the upper ocean. Chap. 10 in Modeling and Prediction of the Upper Layers of the Ocean, (E. B. Kraus, Ed.), Pergamon Press (Oxford).
- Platzman, G. W., 1979: The ENIAC Computations of 1950--Gateway to numerical weather prediction. Bull. Am. Meteor. Soc., 60, 302-312.
- U.S. Naval Weather Service, 1975: Numerical Environmental Products Manual, NAVAIR-1G-522, Naval Weather Service Command, Washington, D.C.
- White, W. B., and R. L. Bernstein, 1979: Design of an oceanographic network in the midlatitude North Pacific. J. Phys. Oceanogr., 9, 592-606.

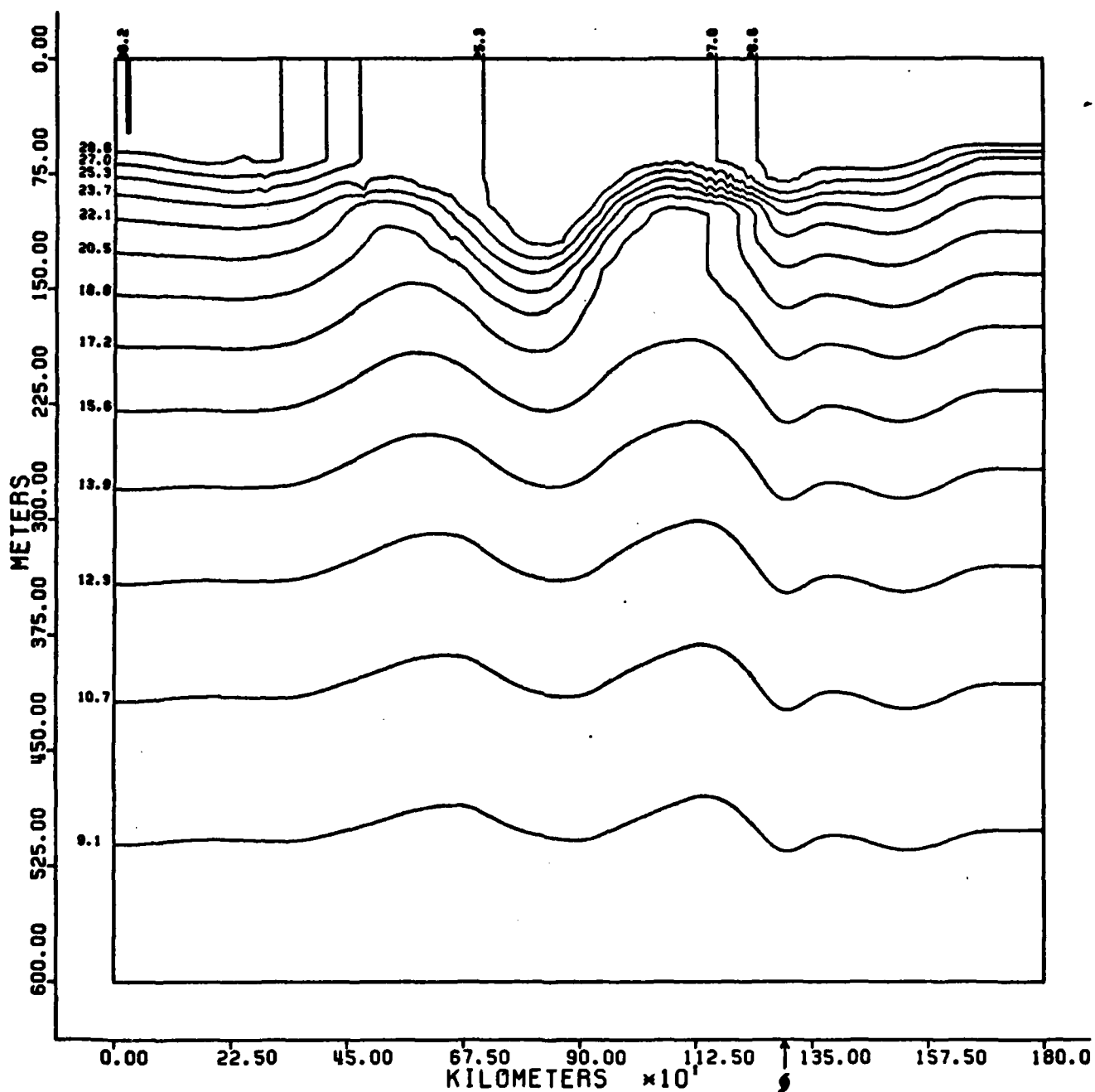


Figure 1. Ocean temperature distribution predicted using an embedded mixed layer model within an ocean circulation model. Cross-section is aligned along the track of the model storm which was located at 450 km at the initial time and has moved toward the right at  $5 \text{ m s}^{-1}$  and is at 1319 km after 48 h.

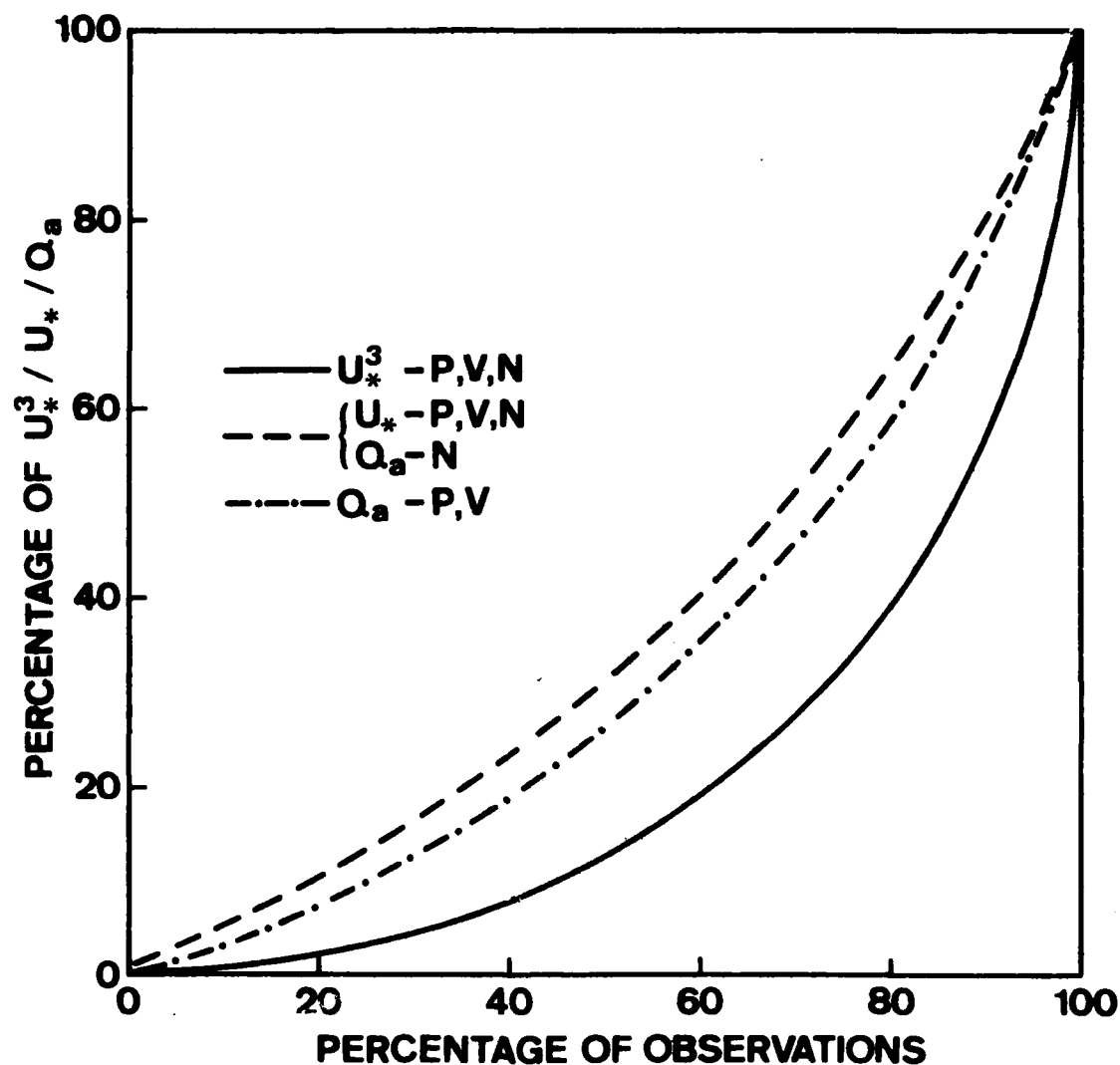


Figure 2. Cumulative percentage of rank-ordered 3 h  $u_*$ ,  $u_*^3$  and  $Q_a$  values versus cumulative percentage of observations based on 24-, 15- and 23-year samples (September to December) at OWS P, V and N, respectively.

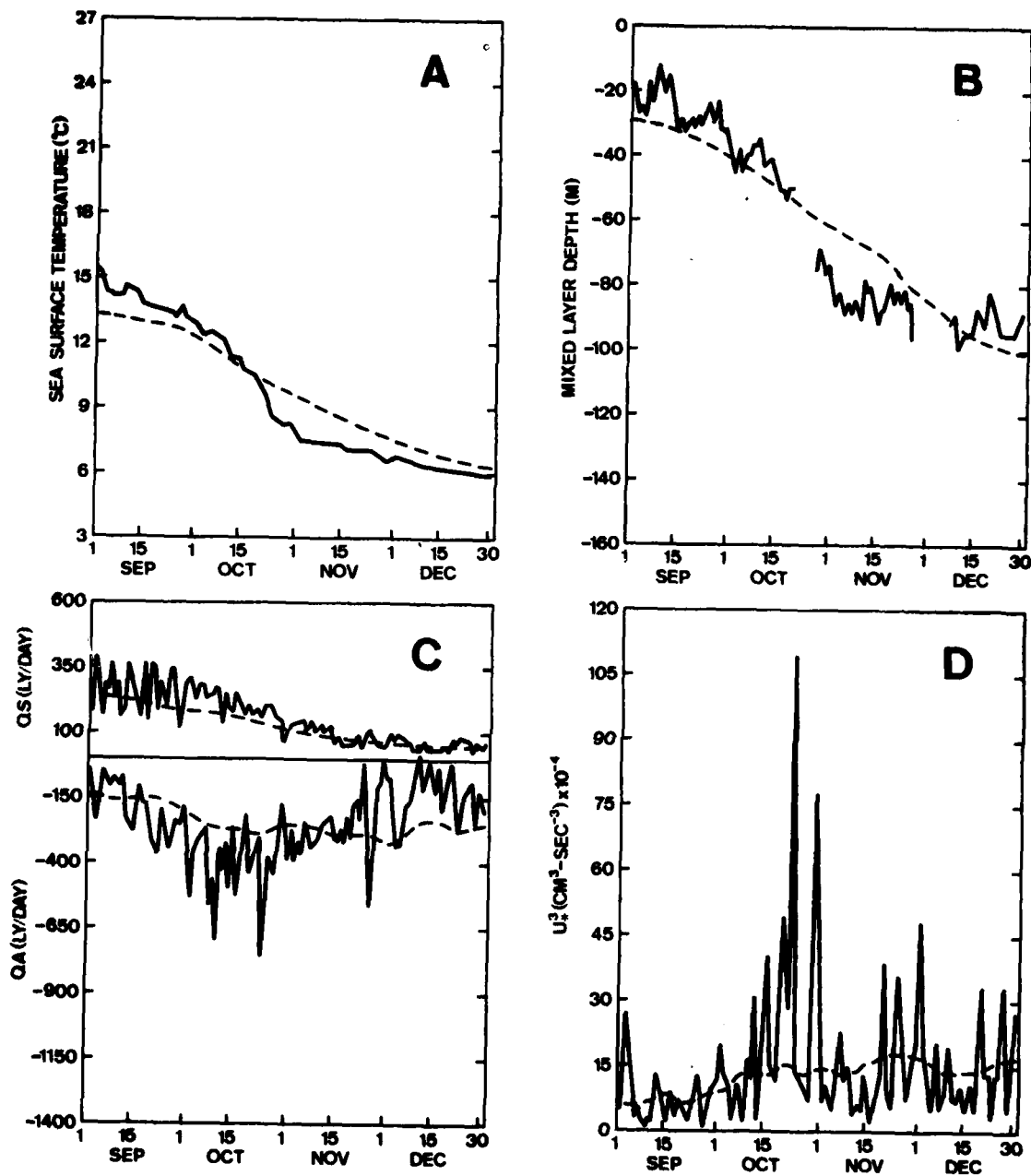


Figure 3. Daily-averaged values of (A) sea-surface temperature, (B) mixed layer depth, (C) insolation ( $Q_s$ ) and surface heat flux plus back radiation ( $Q_g$ ), and (D)  $u_*^3$  at OWS P during 1963. Dashed lines represent the long-term mean (24 year) values.

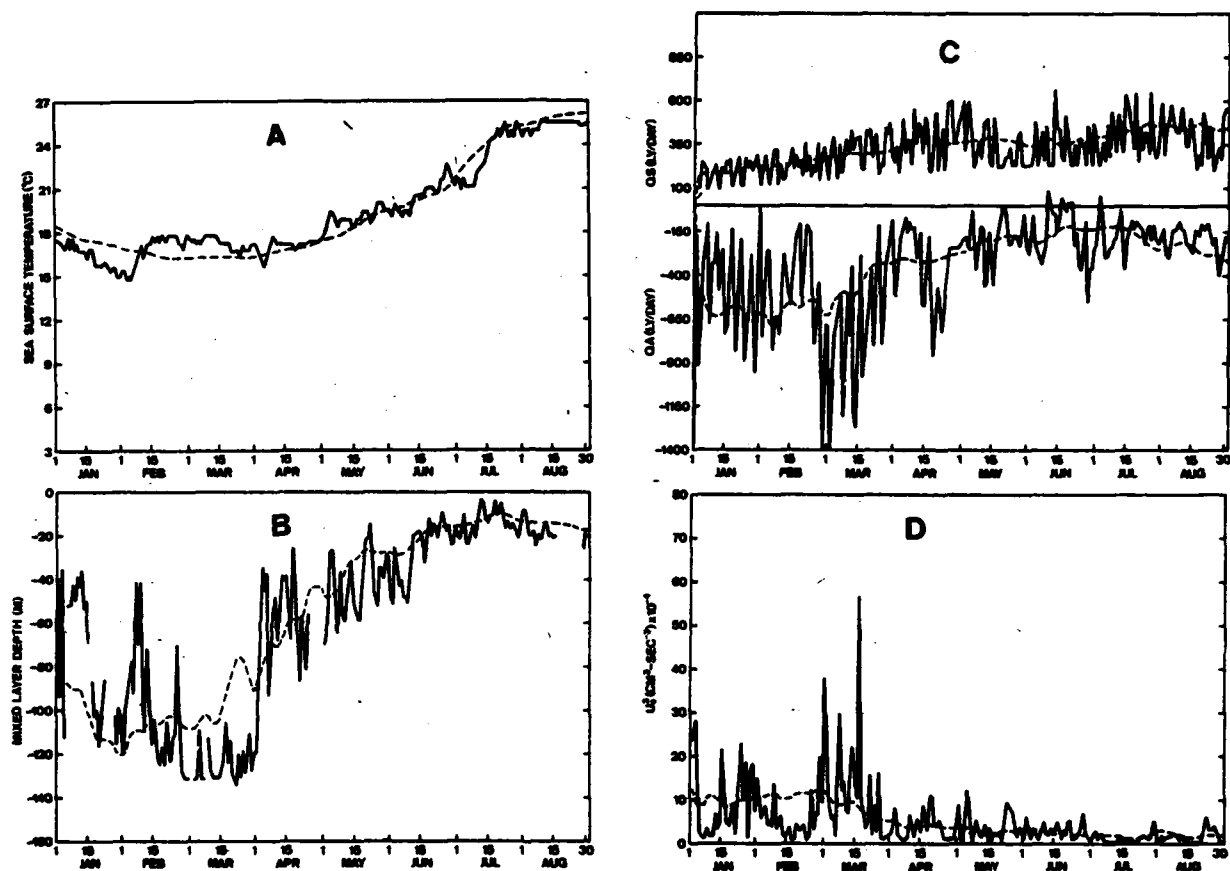


Figure 4. Similar to Fig. 3 except at OWS V during 1959.



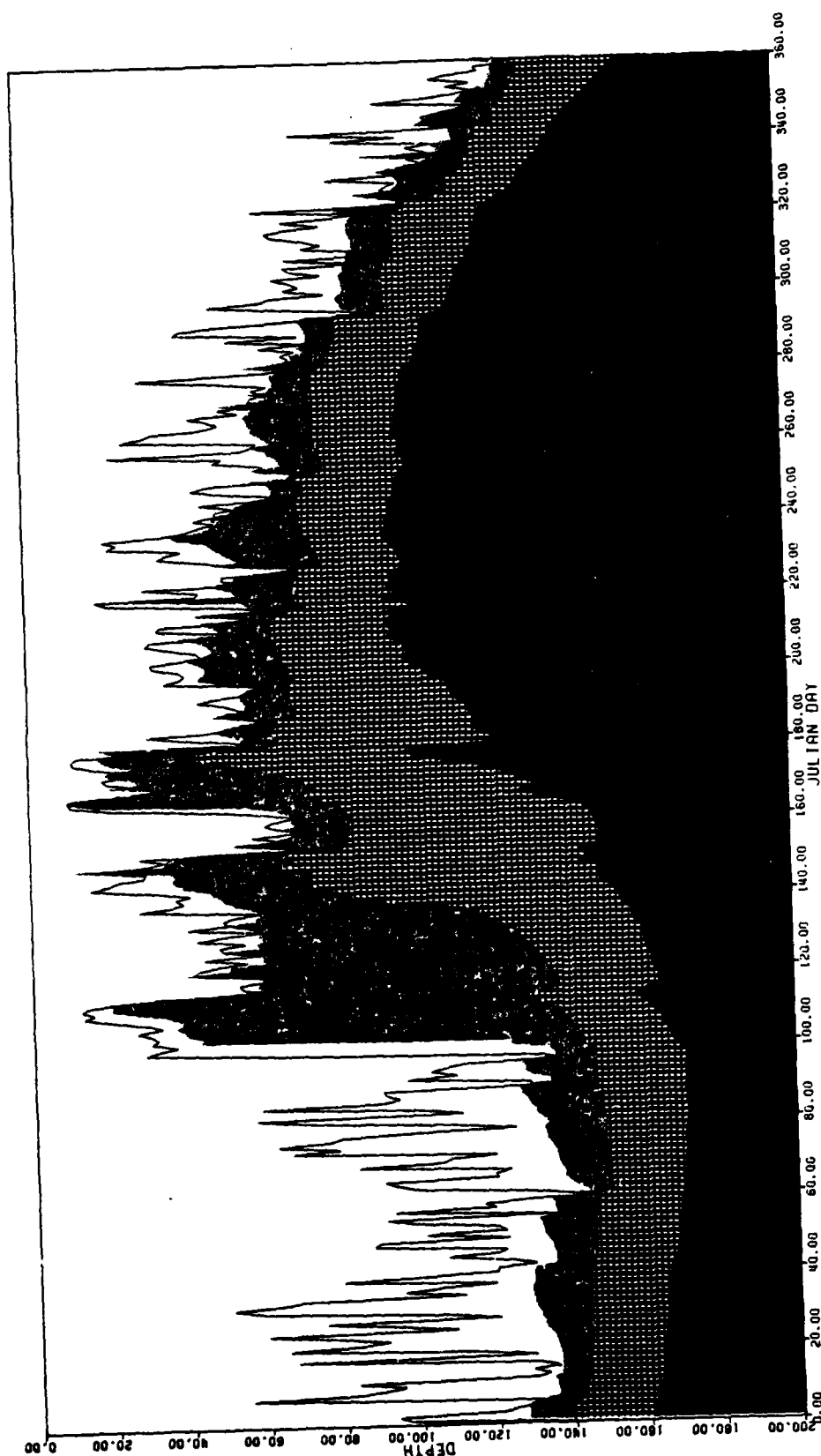


Figure 5. Model-predicted maximum daily depths of the well-mixed layer (solid), surface temperature minus  $0.2^{\circ}\text{C}$  (top of shaded), surface temperature minus  $1.0^{\circ}\text{C}$  (top of cross-hatching) and surface temperature minus  $2.5^{\circ}\text{C}$  (bottom of cross-hatching) during 1959 at OWS P.

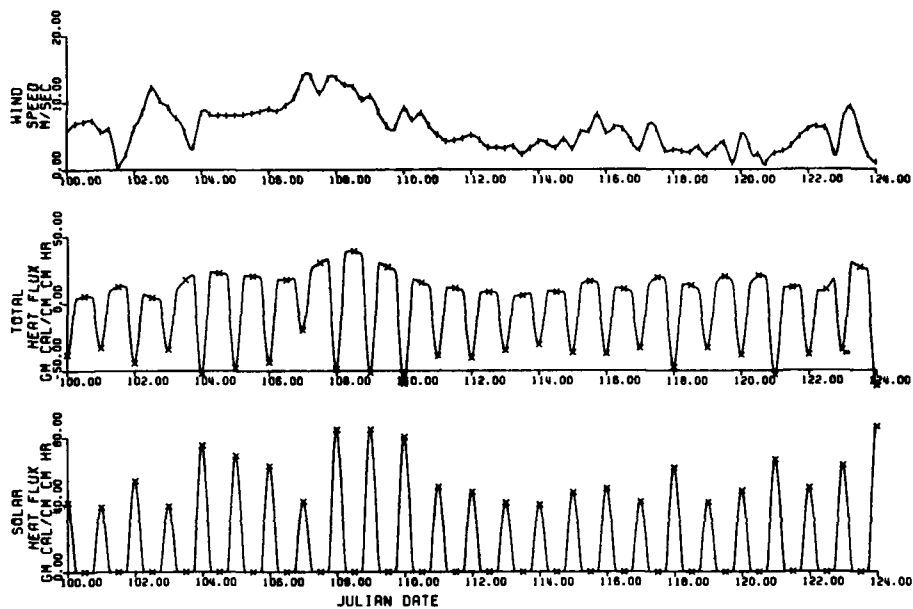


Figure 6. Wind speed, total heat flux and solar heat flux at 32N, 175W during 1977 extracted from FNOG atmospheric model analyses and 12 h predictions.

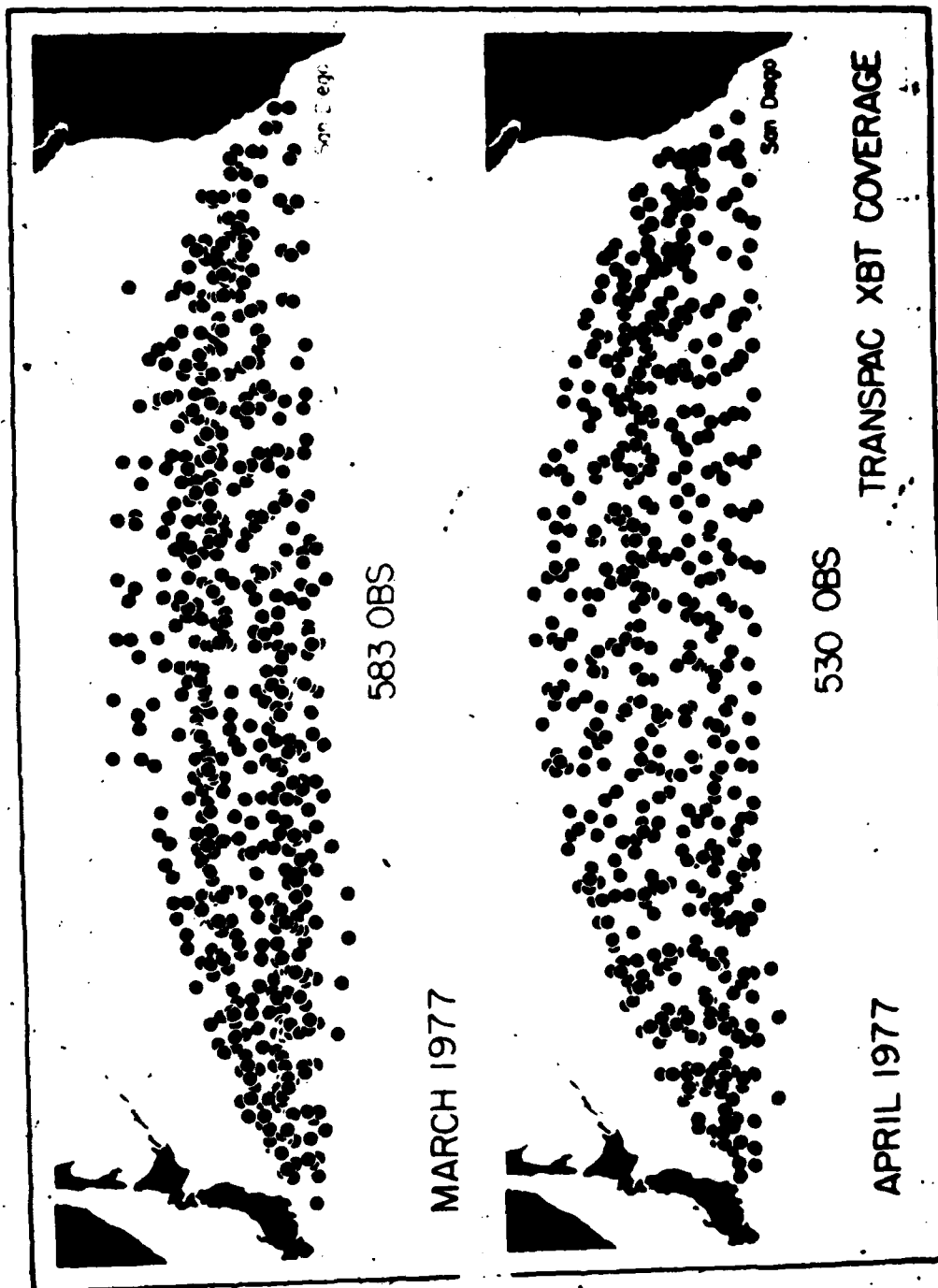


Figure 7. Location of TRANSPAC ship-of-opportunity bathythermograph observations during March and April 1977 (provided by W. White and R. Bernstein).

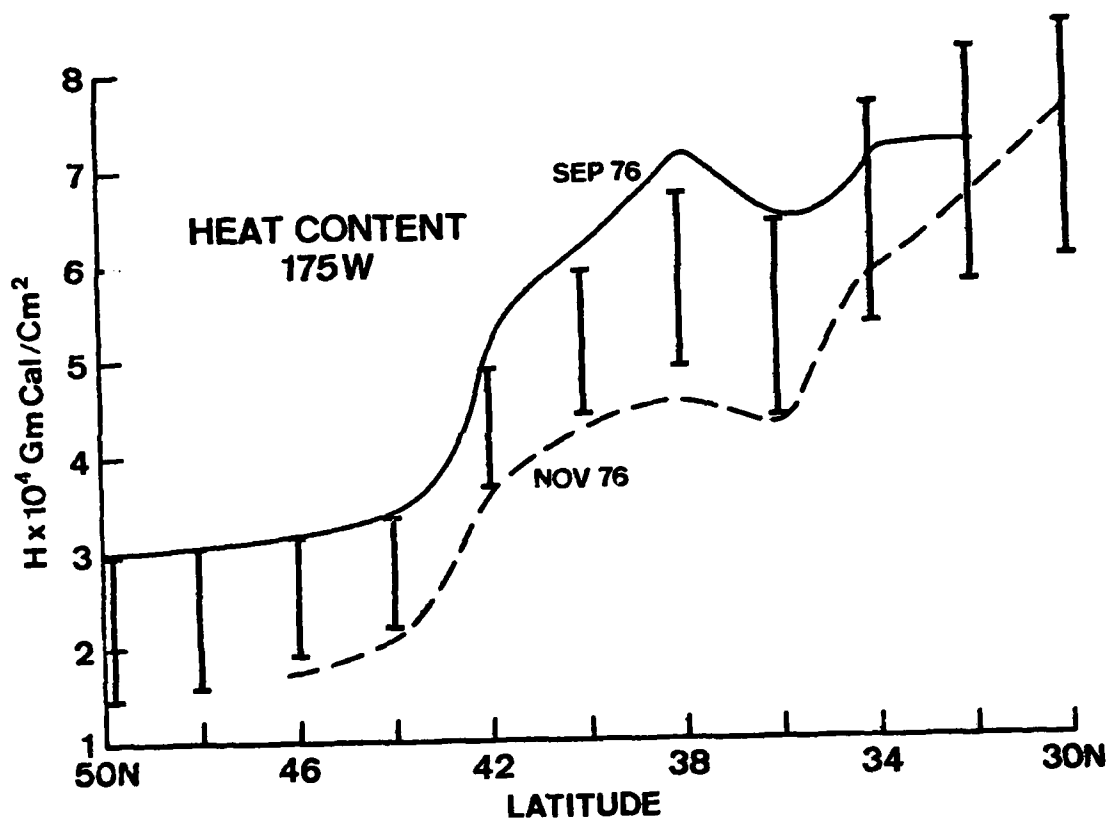


Figure 8. Heat content ( $10^4 \text{ cal cm}^{-2}$ ) relative to the 200 m temperature calculated along  $175^\circ\text{W}$  from TRANSPAC analyses in September (solid) and November (dashed) 1976. Vertical bars indicate the cumulative surface heat flux between 15 September and 15 November 1976.

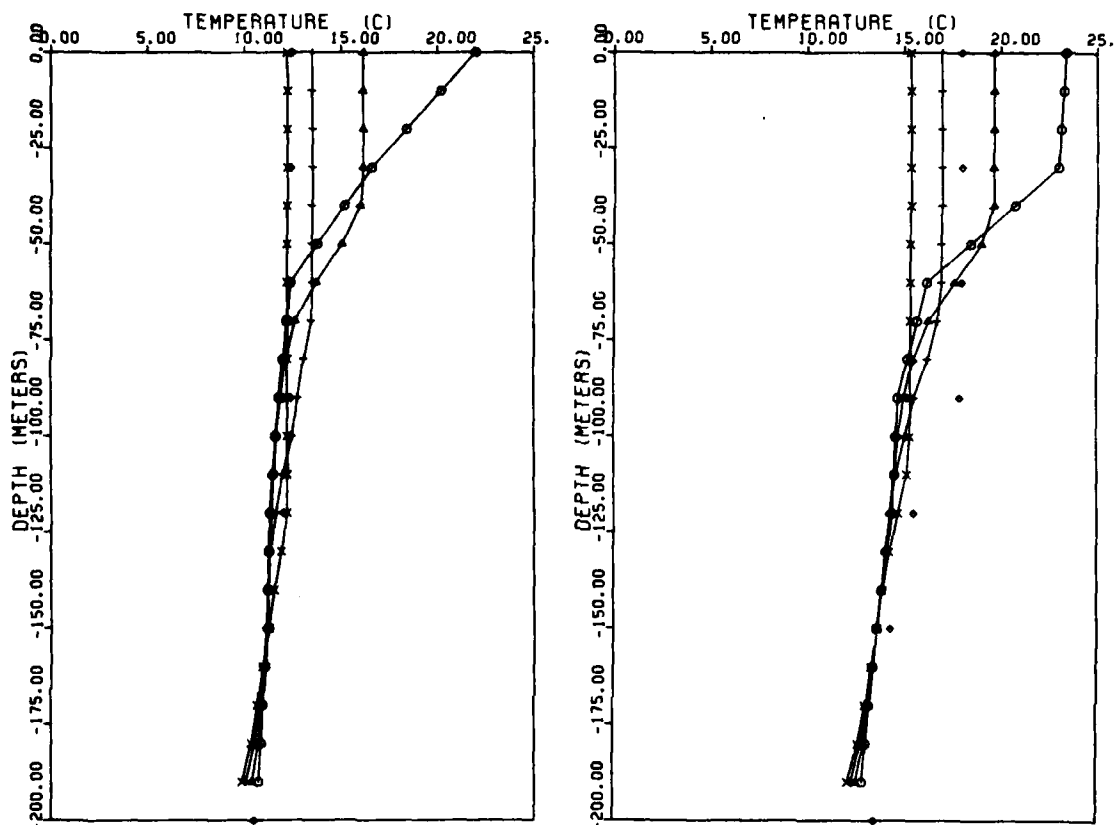


Figure 9. Initial (circles) temperature profiles at (a)  $38^{\circ}\text{N}$ ,  $165^{\circ}\text{W}$  and (b)  $32^{\circ}\text{N}$ ,  $175^{\circ}\text{W}$  from September 1976 TRANSPAC analysis and mean predicted values at 10 m intervals for months of October (triangle), November (horizontal dash) and December 1976 (cross). Verification data from December 1976 TRANSPAC analysis are given at 0, 30, 60, 90, 120, 150 and 200 m (diamond).

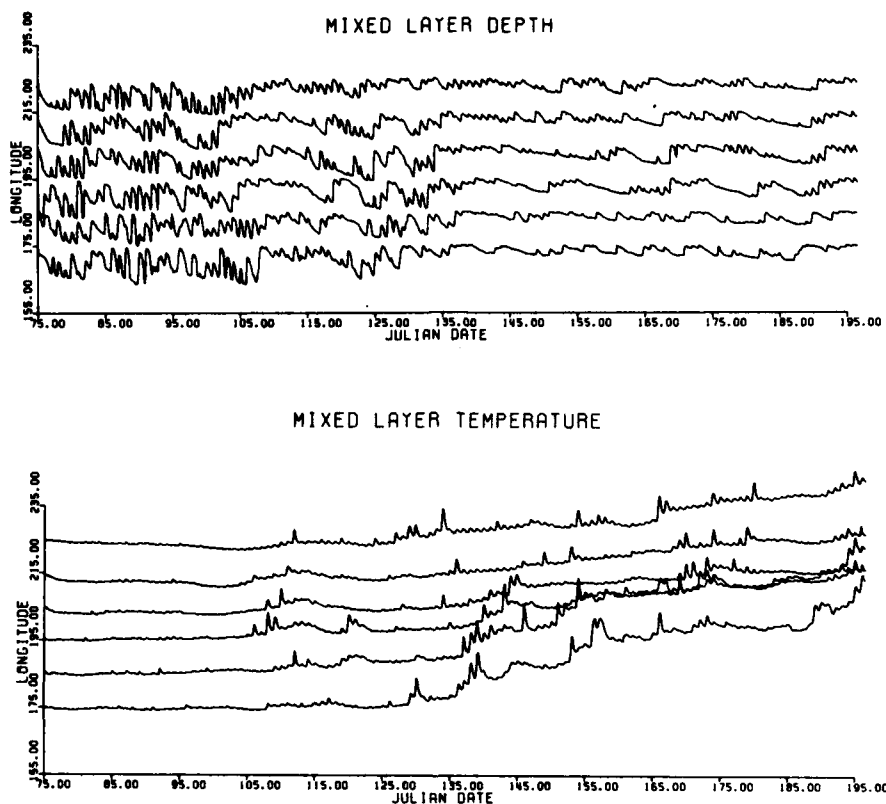


Figure 10. Model-predicted layer (a) depth and (b) temperature during 1976 along 38N. Initial spacing between the traces at each longitude are 100 m and  $2^{\circ}$ , respectively.

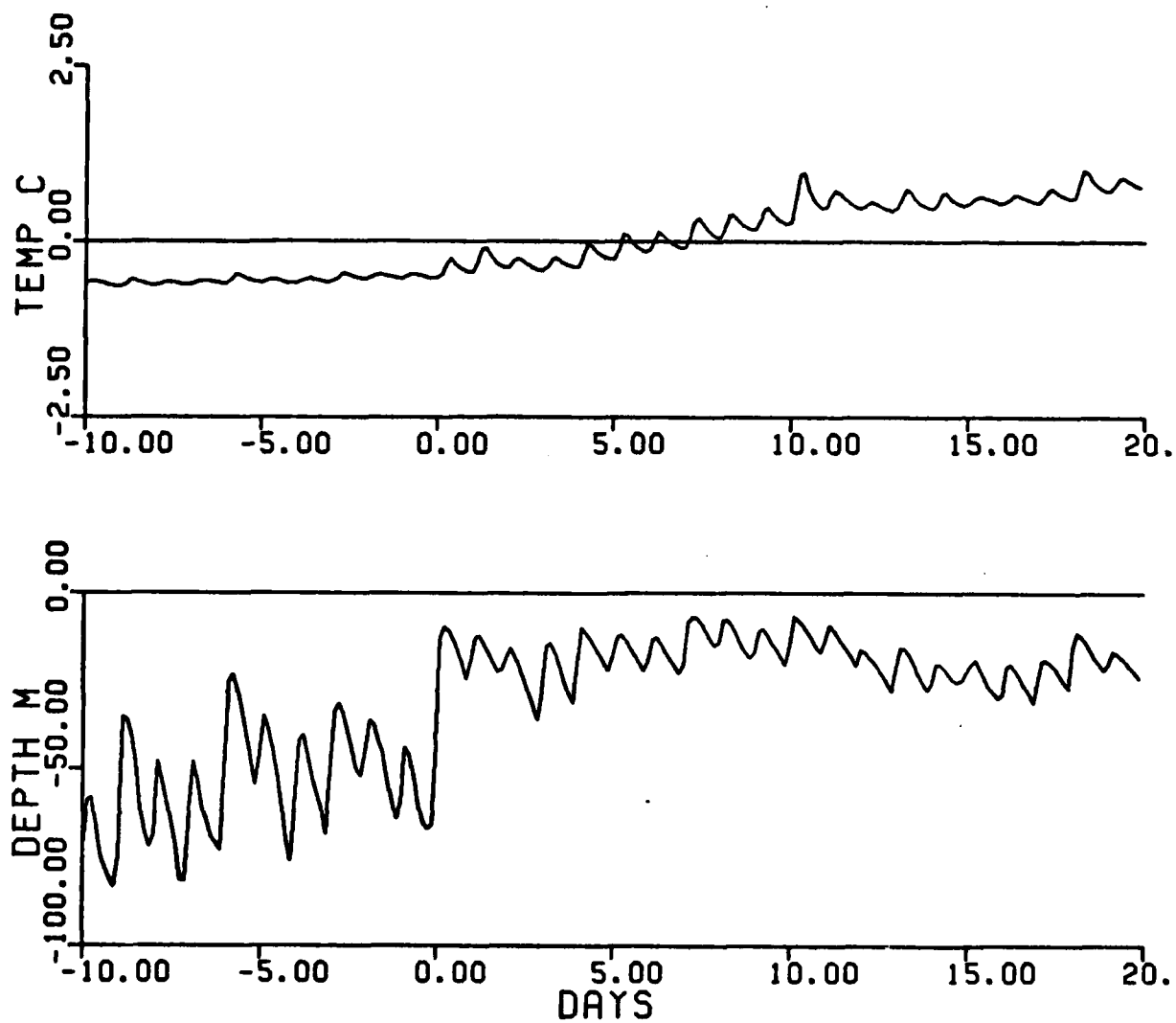


Figure 11. Composite of model-predicted mixed layer temperature (upper) and depth (lower) for 6 longitudes as in Fig. 10, relative to spring transition date (zero day).

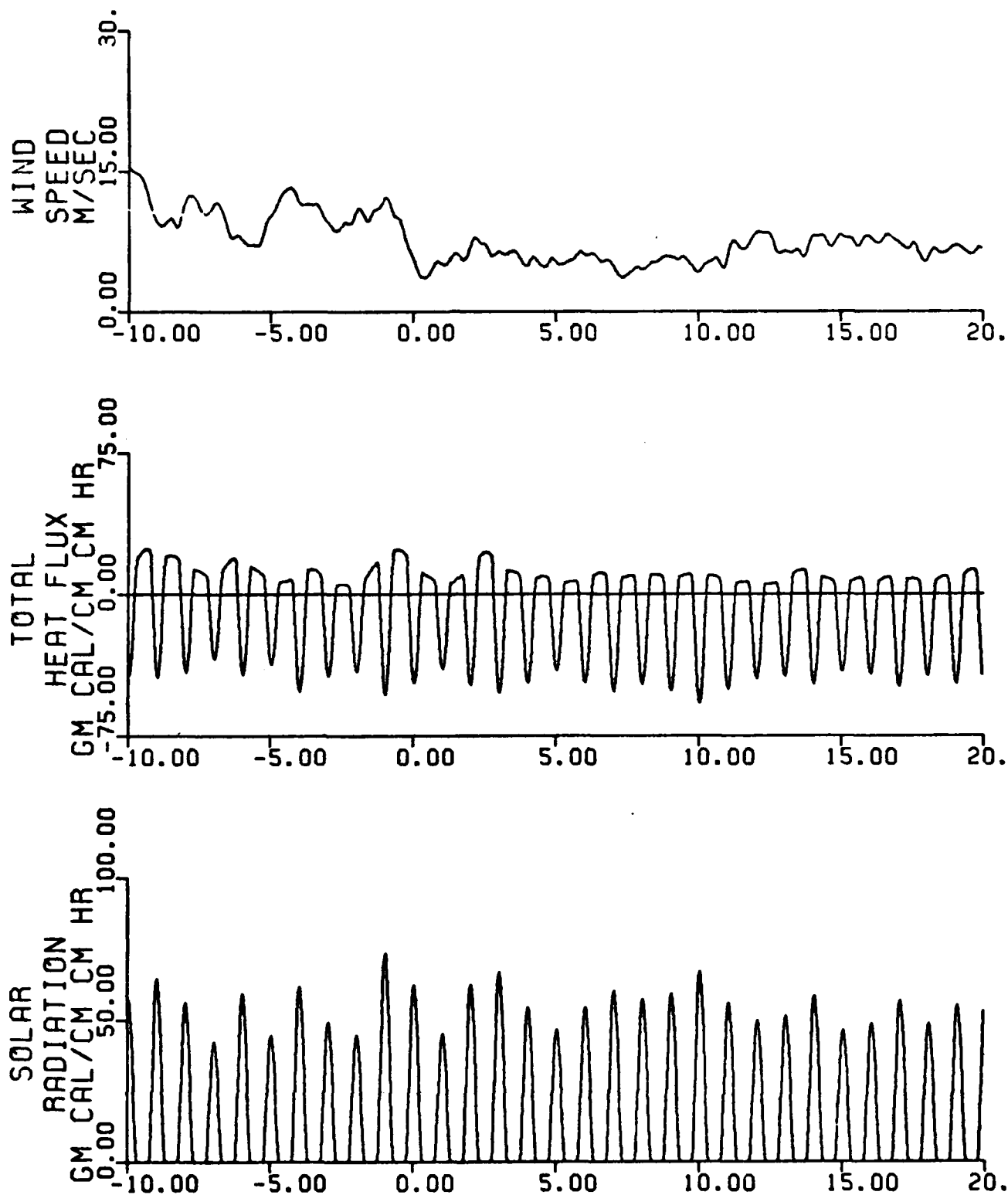


Figure 12. Composite of atmospheric forcing parameters relative to spring transition date as in Fig. 11. Wind speed, total heat flux and solar heat flux are extracted from FNOC atmospheric model analyses and 12-h predictions.



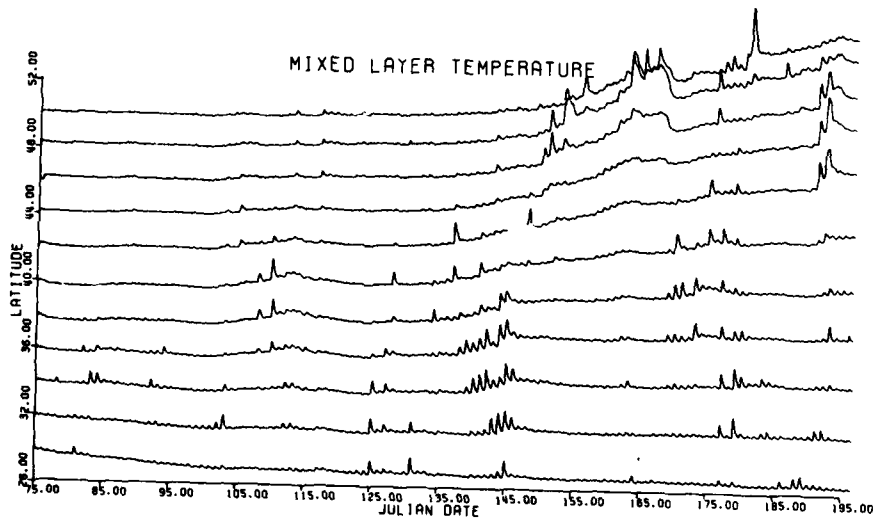
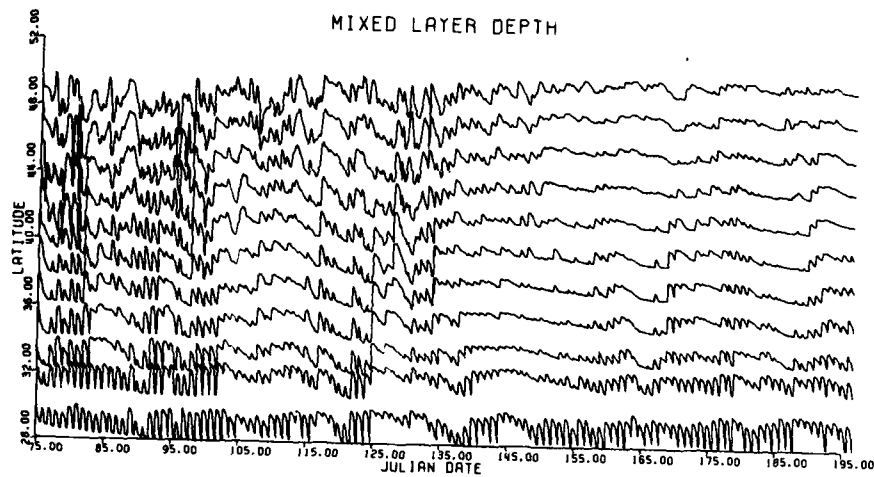


Figure 13. Model-predicted mixed layer depth and temperature as in Fig. 10 except along 155W during 1976.

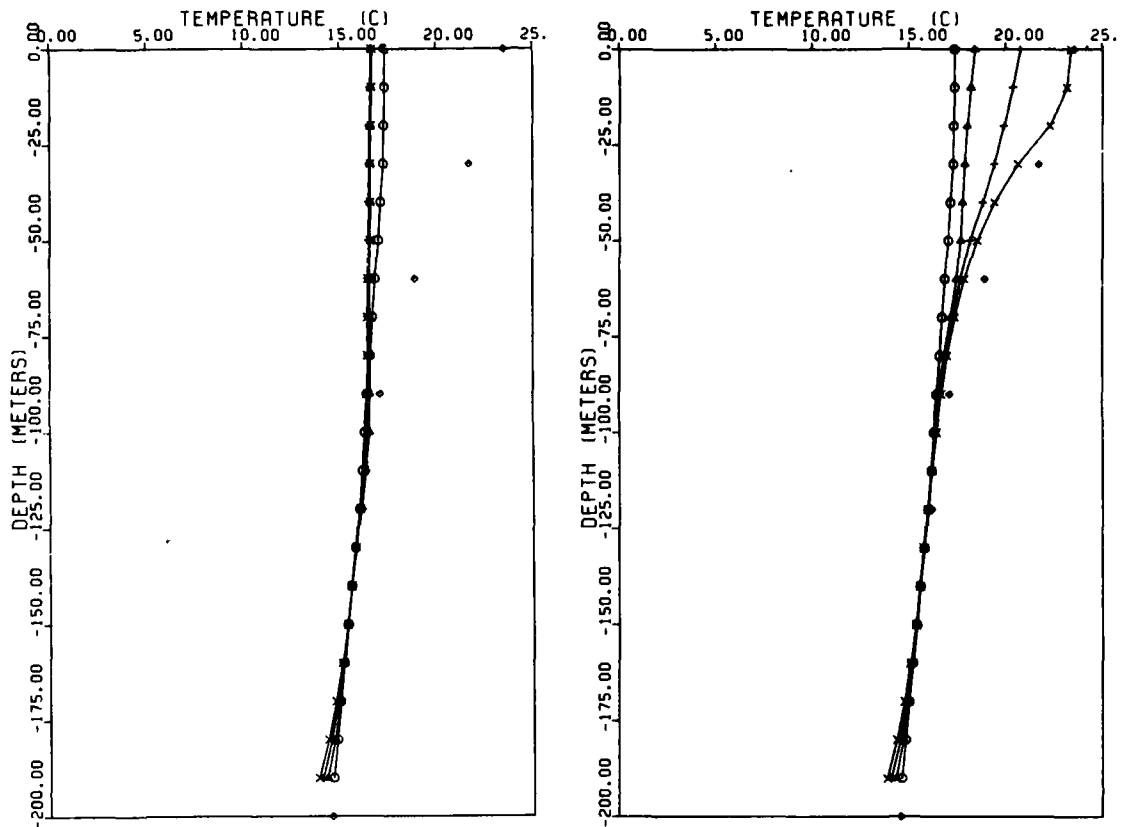


Figure 14. Model predictions as in Fig. 9 except at 30N, 175W and for March (circle), April (triangle), May (horizontal dash) and June (cross) 1977. Verification data are from June 1977 TRANSPAC analysis. (a) Unmodified surface heat flux and (b) reduction of upward heat flux by  $10 \text{ cal cm}^{-2} \text{ h}^{-1}$ .

# DISTRIBUTION LIST

1. Defense Documentation Center Cameron Station Alexandria, VA 22314	2
2. Library, Code 0142 Naval Postgraduate School Monterey, CA 93940	2
3. Commanding Officer (Attn: S. Piacsek) Naval Ocean Research and Development Agency NTSL Station, MS 39529	10
4. Commander Naval Oceanography Command NTSL Station, MS 39529	1
5. Commanding Officer Fleet Numerical Oceanography Center Monterey, CA 93940	1
6. Officer-in-Charge Naval Environmental Prediction Research Facility Monterey, CA 93940	1
7. Commander Naval Oceanographic Office NSTL Station Bay St. Louis, MS 39522 Attn: Code 8100 Attn: Code 6000 Attn: Code 3300	1 1 1
8. Office of Naval Research Code 481 NTSL Station, MS 39529	1
9. Dean of Research, Code 012 Naval Postgraduate School Monterey, CA 93940	2
10. Prof. R. L. Elsberry, Code 63Es Naval Postgraduate School Monterey, CA 93940	10
11. Prof. R. W. Garwood, Jr., Code 68Gd Naval Postgraduate School Monterey, CA 93940	2
12. Department of Meteorology, Code 63 Naval Postgraduate School Monterey, CA 93940	1

- |     |  |             |
|-----|--|-------------|
| 13. | P. C. Gallacher, Code 63Ga<br>Naval Postgraduate School<br>Monterey, CA 93940  | 1           |
| 14. | Department of Oceanography, Code 68<br>Naval Postgraduate School<br>Monterey, CA 93940   | 1           |
| 15. | Commanding Officer<br>Naval Research Laboratory<br>Washington, D.C. 20375<br>Attn: Library, Code 2627  | 6           |
| 16. | Prof. R. L. Haney, Code 63Hy<br>Naval Postgraduate School<br>Monterey, CA 93940  | 1           |
| 17. | Dr. Warren White<br>Scripps Institution of Oceanography A-030<br>La Jolla, CA 92093  | 1           |
| 18. | Dr. Steve Pazan<br>Scripps Institution of Oceanography A-030<br>La Jolla, CA 92093   | 1           |
| 19. | Dr. J. Namias<br>Scripps Institution of Oceanography A-030<br>La Jolla, CA 92093   | 1           |
| 20. | NRL Code 2627<br>Washington, D.C. 20375  | 1           |
| 21. | Office of Naval Research<br>800 N. Quincy Street<br>Arlington, VA 22217<br>Attn: Code 483<br>Attn: Code 460<br>Attn: 102B                                      | 3<br>1<br>2 |
| 22. | Contracting Officer<br>ONR Code 613C: JMD<br>800 N. Quincy Street<br>Arlington, VA 22217   | 1           |
| 23. | Deputy UnderSecretary of Defense<br>(Research and Advanced Technology)<br>Military Assistant for Environmental Science<br>Room 3D120<br>Washington, D.C. 20301 | 1           |
| 24. | NODC/NOAA<br>Code D781<br>Wisconsin Avenue, N.W.<br>Washington, D.C. 20235   | 1           |
| 25. | Commanding Officer<br>ONR Branch Officer<br>Attn: Dr. R. L. Lau<br>1030 East Green Street<br>Pasadena, CA 91106  | 1           |